Design and Fabrication of a Plastic-Free Antenna on a Sustainable Chitosan Substrate

Ilaria Marasco, G. Niro, G. de Marzo, F. Rizzi, A. D'orazio, *Member, IEEE*, M. Grande, *Member, IEEE*, and M. De Vittorio, *Senior Member, IEEE*

***Abstract*— The majority of wearable and flexible 5G and 6G devices are based on plastic substrates, that are harmful to the environment. Therefore, the development of sustainable and plastic-free radio frequency (RF) devices becomes a crucial issue. In this regard, we present a fully biocompatible Planar Inverted-F Antenna (PIFA), fabricated on a 55 μm-thick chitosan substrate. Chitosan has a relative dielectric constant of 5. This antenna is working at 4.5 GHz in the sub-6 GHz band of the 5G spectrum. It has a very compact footprint of 14 x 23 mm^2 and a Specific Absorption Rate (SAR) of 0.41 W/kg. The prototype has been fabricated using an innovative fabrication protocol. A very good agreement between numerical and experimental results has been obtained. The measured realized gain is equal to 1 dBi at the resonant frequency. Our results demonstrate the suitability of chitosan as a dielectric substrate for the fabrication of plastic-free antennas and paves the way for the development of sustainable wearable devices for the Internet of Healthcare Things (IoHT) applications.**

***Index Terms*— Plastic-free antennas, sustainable devices, biocompatible chitosan substrate, sub-6GHz band, IoHT, wearable devices.**

I. Introduction

THE 5G and new 6G communication networks are opening interesting perspectives for wearable and wireless sensor nodes and are very promising for enhancing sensor capabilities [1], [2]. New conceptions of sensing systems imply very compact footprints and connection capabilities to: minimize the impact of the devices, allow the sharing of data, and increase their flexibility. From this perspective, the development of flexible electronics represents a crucial step forward to enhance the wearability and robustness of new devices. In particular, the development of flexible antennas is an open issue which can have disruptive consequences in the fabrication of smart and low-invasive systems.

In this frequency range, the standard de facto regarding flexible antennas is represented by microstrips, due to their exceptional properties combined with straightforward manufacturing production techniques [3]. However, the connected and flexible radio frequency systems have disadvantages. The increasing use of halogenated or toxic compounds are harmful to the environment. The employment of the polluting plastic-based flexible substrates such as Kapton [4], Polyethylene Naphtalate (PEN) [5], [6], [7], Polyethylene Terephthalate (PET) [8], and Liquid Crystal Polymers (LCPs) [9], [10].

In this scenario, the development of flexible and biocompatible plastic-free antennas becomes a crucial challenge to open new applications in the quest for sustainability-conscious technology development. One of the main choices regarding flexible antennas is represented by textiles. The precise printing of the metallic layer presents several challenges related to the high deformability of these kinds of materials. Alternatively, L. Andre et al. proposed a manufacturing process based on the lamination technique, in which the radiative element is placed on a plastic polyimide layer, and the dielectric substrate is manufactured in parallel and attached using glues [11]. Embroidered antennas [12], [13] can be obtained using conductive yarns having low conductivity. Therefore, these antennas present radiation efficiencies and gain lower than other types of antennas.

An alternative solution commonly found in the literature is represented by photographic paper-based antennas [14], [15]. These substrates are obtained using complex fabrication processes and characterized by thicknesses in the range of 200-400 μm. Their adhesion with the metal layers is very poor, so some cracks after bending can happen. Furthermore, these substrates are not optically transparent. Among nature-derived polymers, chitosan displays a combination of advantageous properties. It is a biocompatible material, according to in vitro tests, which can be easily extracted at low cost from numerous sources, such as shrimp shells [16]. Another important feature of this material is its optical transparency, which can reduce the visual impact by camouflaging the antenna.

Manuscript received 21 December 2022; accepted 27 December 2022. Date of publication 28 December 2022; date of current version 27 January 2023. The review of this letter was arranged by Editor H. Lee. *(Ilaria Marasco, G. Niro, and G. de Marzo contributed equally to this work.) (Corresponding author: Ilaria Marasco.)*

Ilaria Marasco and G. Niro are with the Department of Electrical and Information Engineering, Politecnico di Bari, 70125 Bari, Italy, and also with the Center for Biomolecular Nanotechnologies, Istituto Italiano di Tecnologia, Arnesano, 73010 Lecce, Italy (e-mail: ilaria.marasco@poliba.it).

G. de Marzo and F. Rizzi are with the Center for Biomolecular Nanotechnologies, Istituto Italiano di Tecnologia, Arnesano, 73010 Lecce, Italy.

A. D'orazio and M. Grande are with the Department of Electrical and Information Engineering, Politecnico di Bari, 70125 Bari, Italy.

M. De Vittorio is with the Department of Engineering and Innovation, Università del Salento, 73100 Lecce, Italy, and also with the Center for Biomolecular Nanotechnologies, Istituto Italiano di Tecnologia, Arnesano, 73010 Lecce, Italy.

Color versions of one or more figures in this letter are available at https://doi.org/10.1109/LED.2022.3232986.

Digital Object Identifier 10.1109/LED.2022.3232986

This work is licensed under a Creative Commons Attribution-NonCommercial-NoDerivatives 4.0 License.
For more information, see https://creativecommons.org/licenses/by-nc-nd/4.0/

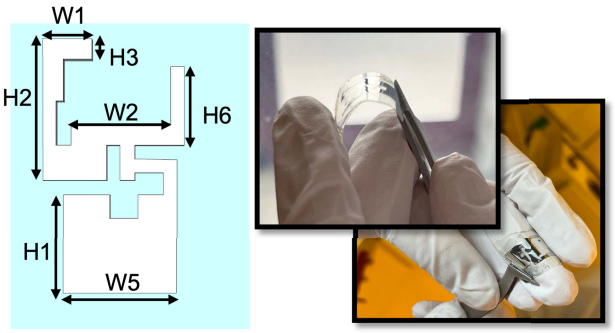

Fig. 1. Antenna overview: a) Sketch of the simulated antenna, b) fabricated prototype.

Chitosan obtained with this protocol also presents optimal piezoelectric properties suggesting its use in complex systems integrating radiofrequency antennas with microelectromechanical transducers (MEMs) [17], [18]. The exploitation of chitosan-based biocompatible materials in a wearable antenna whose Specific Absorption Rate (SAR) is lower than the maximum threshold allows envisioning the design and realization of an Internet of Healthcare Things (IoHT) biosensor node. Despite its optimal properties, to the best of our knowledge chitosan-based antennas working in the sub-6GHz band have not yet been reported in the literature.

In this work, we propose the design and fabrication of a Planar Inverted- F Antenna (PIFA) on a 55 μm-thick chitosan substrate. The radiative part of the antenna is made of biocompatible silver nanoparticle ink. It is fabricated implying a novel and innovative approach developed for thin microwave devices [16]. The developed prototype has a very compact footprint of 14×23 mm^2 and it works in the sub-6GHz of 5G spectrum at a frequency of 4.5 GHz. Finally, it has been characterized in terms of scattering parameter S_{11} using Vector Network Analyzer (VNA) and 2D radiation pattern.

II. Design and Simulations

The schematic diagram of the proposed antenna is reported in Figure 1 a). The light blue part represents the dielectric substrate, whereas the white portion is the radiative element. The overall dimensions are 14×23 mm^2. The antenna is composed of two L-shape regions: W1xH2 (3.5×10 mm) responsible for the resonant tuning of the resonant frequency and W2xH6 (7×3 mm), responsible for the impedance matching at 50 Ω. The width of the strips is equal to H3 (1 mm). The portion W5xH1 (8×6 mm) represents the ground plane whereas the region in the middle of the device is used as feeding point in which we put the 3D model of an U.FL connector.

The device has been placed on a 55 μm-thick chitosan substrate that has a relative dielectric constant of 5 in 3 – 6 GHz range [15].

PIFA has been simulated by means of a Finite Difference Time Domain (FDTD) solver. The scattering parameter S_{11} and radiation patterns for E-plane and H-plane have been calculated. The simulated results are shown in Figure 2 a)-c). In figure 2a) the trend of the simulated scattering parameter

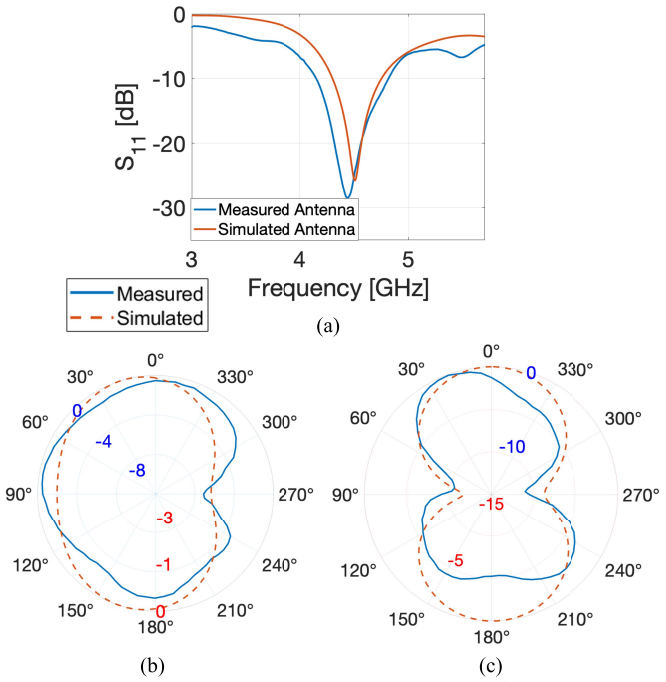

Fig. 2. Comparison between simulated (red curve) and measured (blue curve) for: a) scattering parameter S_{11}, b) 2D polar plot for the plane $\Phi = 0°$, c) 2D polar plot for the plane $\Phi = 90°$ at the resonant frequency.

S_{11} (red curve) is reported: there is a dip of -26 dB at 4.5 GHz with a bandwidth of about 450 MHz. In Figure 2 b) and 2 c) the polar plots of the radiation pattern for E-plane ($\Phi = 0°$) and H-plane ($\Phi = 90°$) at the resonant frequency are shown. For $\Phi = 0°$, the main lobe magnitude is equal to 1.33 dBi and the main lobe direction is equal to 15.0 deg. Whereas for the $\Phi = 90°$ the main lobe magnitude is equal to 1.27 dBi and the main lobe direction is equal to 0 deg.

The maximum value of the realized gain at 4.5 GHz is equal to 1.38 dBi. Further analysis has been performed for the evaluation of the SAR, to investigate the possibility to place the antenna on the human body. The simulations for SAR results have been carried on a simplified model composed of four layers (i.e. bone, muscle, fat and skin) [19], [20]. The result of the analysis performed on 10 g of tissue shows that the SAR value at the resonant frequency of 4.5 GHz is equal to 0.41 W/kg, well under the European limit of 2 W/kg.

III. Fabrication and Characterization

The PIFA has been fabricated using an innovative fabrication protocol (Figure 3) developed for thin devices and implemented to fabricate the presented antenna.

The preliminary step is the fabrication of the chitosan substrate. An aqueous solution with 1 % w/v of Chitosan (890000 avg M. W., Glentham) and 1 % v/v of Lactic Acid (Sigma Aldrich) is stirred until the polymer is dissolved. Then, 40 mL of the solution are poured into a glass Petri dish and left to dry overnight at 200 mbar and 40°C. According to the protocol described in the literature, the film is then soaked in NaOH 1 M for 60 minutes and then washed with water until the pH of the washing water is 7. Finally, the film is peeled off from the Petri dish and ready to be employed for the

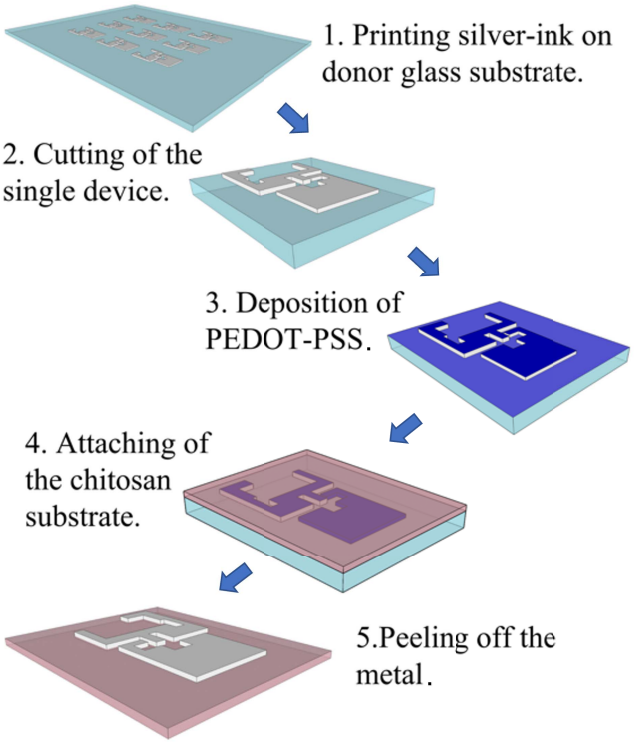

Fig. 3. Fabrication steps.

fabrication of the antenna. To avoid impurity contamination, all the steps are performed in a clean room.

After the synthesis of the substrate, the protocol goes on with the fabrication of the antenna prototype. The first step is the deposition of the Silver- based ink on a donor glass by means of NanoDimension's Dragonfly LDM multi-material 3D printer. The antenna has been printed with a thickness of 35 μm in order to guarantee the optimal conductivity of the ink (the minimum threshold is fixed at 17 μm). The process has been performed at 140°C to allow a proper sintering of the ink and then, in less than two hours, 25 antennas have been printed. The fabrication protocol continues by cutting each single antenna from the glass sheet with a diamond tool. The third step is the functionalization of the surface with the deposition of an interlayer of PEDOT: PSS/ Glycerol. A 200 nm thick layer has been spin-coated on the surface to guarantee an optimal adhesion between the Silver-based ink and the chitosan substrate. The PEDOT: PSS has been cured for 30 minutes at a temperature of 140°C. The last two steps consist in attaching the dielectric chitosan substrate to the donor glass and then peeling off the metal from it. This last procedure was performed after placing the sample under a vacuum for two hours.

In the end the final prototype has been obtained as shown in Figure 3 a). The U.FL connector has been placed on the feeding point in order to perform the characterization step, the measured results are shown in Figures 2 b)-c).

The device has been characterized in terms of scattering parameter S_{11} by means of a Vector Network Analyzer (VNA) and 2D polar plots for the radiation pattern. In Figure 2 b) the comparison between the measured (blue curve) and simulated (red curve) scattering parameter S_{11} of the antenna is reported. A very good agreement in terms of resonance dip has been found. In addition, the measured curve presents a slightly wide bandwidth with respect to the simulated one. This effect is attributed to three main factors: (i) the metallic losses since the Ag-based ink is a combination of silver nanoparticles and solvent molecules, (ii) the integration of the connector, and, especially, (iii) the soldering and the insertion loss of the U.FL to SMA transition cable. All these effects become more relevant at the resonant frequency because there is a maximum power transfer to the device and consequently a higher dissipation.

TABLE I
COMPARISON BETWEEN FLEXIBLE ANTENNAS

Reference	f_c [GHz]	B.W. [%]	Gain [dBi]	Footprint $[mm^3]$	Plastic Free	Transparent
[4]	5.5	90	-0.4	20x30x0.12	No	No
[14]	2.4	8.4	2.0	40x35x0.6	Yes	No
[15]	2.2/5.35	0.45/2.8	2.0	40x34x0.26	Yes	No
T.W.	4.5	15	1.0	14x23x0.05	Yes	Yes

In Fig. 2b) and c) the comparison between the measured (blue curves) and simulated (red curves) polar plots for the planes phi $= 0°$ and $\phi = 90°$ are shown, respectively. The trends of the radiation patterns are in good agreement for both planes. In general, slightly lower values in the measurements can be observed due to mechanical alignments. In particular, measured radiation pattern for plane $\phi = 0°$ (Fig 2b)), presents a lower minimum value than the simulations. This is due to the presence of the cable in front of the antenna, the losses of the measurements set up and the soldering of the connector. For the $\phi = 90°$ plane, (Fig. 2c)), there is a good agreement also in terms of minimum value, -15 dB for both the measured and the simulated results. The measured value of the gain is 1 dBi at the resonant frequency which is fully in line with the numerical findings.

Table I compares the proposed antenna with other flexible antennas reported in the literature. It is highlighted that the proposed antenna presents a higher bandwidth with respect to the reported plastic-free antennas, whereas the gain is comparable. Finally, it is characterized by a non-invasive and lightweight profile due to its very compact footprint. Furthermore, it is transparent to the visible spectrum.

IV. CONCLUSION

In this letter, we present the design of the first prototype of fully-biocompatible silver-based PIFA placed on a flexible chitosan substrate. The prototype has been fabricated by means of an innovative fabrication protocol in the field of antennas. The measured results show a very good agreement with the predictions made through numerical simulations. The fabricated antennas are characterized by a very high flexibility and transparency of about 80%, showing the potential of chitosan as dielectric substrate in the field of antennas. These results pave the way for the next generation of plastic-free and sustainable health-monitoring devices for IoHT applications.

REFERENCES

[1] M. Agiwal, A. Roy, and N. Saxena, "Next generation 5G wireless networks: A comprehensive survey," *IEEE Commun. Surveys Tuts.*, vol. 18, no. 3, pp. 1617–1655, 3rd Quart., 2016, doi: 10.1109/COMST.2016.2532458.

[2] J. Iannacci and H. V. Poor, "Review and perspectives of micro/nano technologies as key-enablers of 6G," *IEEE Access*, vol. 10, pp. 55428–55458, 2022, doi: 10.1109/ACCESS.2022.3176348.

[3] L.-Y. Ma and N. Soin, "Recent progress in printed physical sensing electronics for wearable health-monitoring devices: A review," *IEEE Sensors J.*, vol. 22, no. 5, pp. 3844–3859, Mar. 2022, doi: 10.1109/JSEN.2022.3142328.

[4] I. I. Labiano and A. Alomainy, "Flexible inkjet-printed graphene antenna on Kapton," *Flexible Printed Electron.*, vol. 6, no. 2, Jun. 2021, Art. no. 025010, doi: 10.1088/2058-8585/ac0ac1.

[5] I. Marasco, G. Niro, F. Rizzi, A. D'Orazio, M. D. Vittorio, and M. Grande, "Dual band flexible planar inverted-F antenna for internet of healthcare things applications," in *Proc. Microw. Medit. Symp. (MMS)*, May 2022, pp. 1–4, doi: 10.1109/MMS55062.2022.9825573.

[6] I. Marasco, G. Niro, V. M. Mastronardi, F. Rizzi, A. D'Orazio, M. D. Vittorio, and M. Grande, "A compact evolved antenna for 5G communications," *Sci. Rep.*, vol. 12, no. 1, Jun. 2022, Art. no. 10327, doi: 10.1038/s41598-022-14447-9.

[7] I. Marasco, G. Niro, L. Lamanna, L. Piro, F. Guido, L. Algieri, V. M. Mastronardi, A. Qualtieri, E. Scarpa, D. Desmaële, F. Rizzi, A. D'Orazio, M. D. Vittorio, and M. Grande, "Compact and flexible meander antenna for surface acoustic wave sensors," *Microelectron. Eng.*, vol. 227, Apr. 2020, Art. no. 111322, doi: 10.1016/j.mee.2020.111322.

[8] S. I. H. Shah and S. Lim, "DNA-inspired frequency reconfigurable origami antenna using segmented rotation technique," *Smart Mater. Struct.*, vol. 30, no. 1, Jan. 2021, Art. no. 015004.

[9] H. Zhang, Y. Lan, S. Qiu, S. Min, H. Jang, J. Park, S. Gong, and Z. Ma, "Flexible and stretchable microwave electronics: Past, present, and future perspective," *Adv. Mater. Technol.*, vol. 6, no. 1, Jan. 2021, Art. no. 2000759, doi: 10.1002/admt.202000759.

[10] M. Venkateswara Rao, B. T. P. Madhav, T. Anilkumar, and B. Prudhvinadh, "Circularly polarized flexible antenna on liquid crystal polymer substrate material with metamaterial loading," *Microw. Opt. Technol. Lett.*, vol. 62, no. 2, pp. 866–874, Feb. 2020, doi: 10.1002/mop.32088.

[11] L. Andre, P. Pinho, C. Gouveia, and C. Loss, "Textile antenna for first-person view goggles," *Elektronika Elektrotechnika*, vol. 27, no. 2, pp. 49–54, Apr. 2021, doi: 10.5755/j02.eie.28841. [Online]. Available: https://eejournal.ktu.lt/index.php/elt/article/view/28841

[12] D. Bonefačić and J. Bartolić, "Embroidered textile antennas: Influence of moisture in communication and sensor applications," *Sensors*, vol. 21, no. 12, p. 3988, Jun. 2021, doi: 10.3390/s21123988. [Online]. Available: https://www.mdpi.com/1424-8220/21/12/3988

[13] C. Loss, R. Gonçalves, C. Lopes, P. Pinho, and R. Salvado, "Smart coat with a fully-embedded textile antenna for IoT applications," *Sensors*, vol. 16, no. 6, p. 938, Jun. 2016, doi: 10.3390/s16060938. [Online]. Available: https://www.mdpi.com/1424-8220/16/6/938

[14] M. Ullah, M. Islam, T. Alam, and F. Ashraf, "Paper-based flexible antenna for wearable telemedicine applications at 2.4 GHz ISM band," *Sensors*, vol. 18, no. 12, p. 4214, Dec. 2018, doi: 10.3390/s18124214. [Online]. Available: https://www.mdpi.com/1424-8220/18/12/4214

[15] H. F. Abutarboush, "Silver nanoparticle inkjet-printed multiband antenna on synthetic paper material for flexible devices," *Alexandria Eng. J.*, vol. 61, no. 8, pp. 6349–6355, Aug. 2022, doi: 10.1016/j.aej.2021.11.060.

[16] G. de Marzo, V. M. Mastronardi, L. Algieri, F. Vergari, F. Pisano, L. Fachechi, S. Marras, L. Natta, B. Spagnolo, V. Brunetti, F. Rizzi, F. Pisanello, and M. D. Vittorio, "Sustainable, flexible, and biocompatible enhanced piezoelectric chitosan thin film for compliant piezosensors for human health," *Adv. Electron. Mater.*, Mar. 2022, Art. no. 2200069, doi: 10.1002/aelm.202200069.

[17] X. Yang and M. Zhang, "Review of flexible microelectromechanical system sensors and devices," *Nanotechnol. Precis. Eng.*, vol. 4, no. 2, Jun. 2021, Art. no. 025001, doi: 10.1063/10.0004301.

[18] G. Niro, I. Marasco, F. Rizzi, A. D'Orazio, M. D. Vittorio, and M. Grande, "Design of a surface acoustic wave resonator for sensing platforms," in *Proc. IEEE Int. Symp. Med. Meas. Appl. (MeMeA)*, Jun. 2020, pp. 1–6, doi: 10.1109/MeMeA49120.2020.9137116.

[19] M. S. Wegmueller, A. Kuhn, J. Froehlich, M. Oberle, N. Felber, N. Kuster, and W. Fichtner, "An attempt to model the human body as a communication channel," *IEEE Trans. Biomed. Eng.*, vol. 54, no. 10, pp. 1851–1857, Oct. 2007, doi: 10.1109/TBME.2007.893498.

[20] Y. Song, Q. Hao, K. Zhang, M. Wang, Y. Chu, and B. Kang, "The simulation method of the galvanic coupling intrabody communication with different signal transmission paths," *IEEE Trans. Instrum. Meas.*, vol. 60, no. 4, pp. 1257–1266, Apr. 2011, doi: 10.1109/TIM.2010.2087870.

Open Access funding provided by 'Istituto Italiano di Tecnologia' within the CRUI CARE Agreement